11B

PNL-2938
UC-79e

COBRA-IV Wire Wrap Data Comparisons

T. E. Donovan
T. L. George
C. L. Wheeler

February 1979

Prepared for the U.S. Department of Energy
under Contract EY-76-C-06-1830

Pacific Northwest Laboratory
Operated for the U.S. Department of Energy
by Battelle Memorial Institute

Battelle

PNL-2938

NOTICE

PACIFIC NORTHWEST LABORATORY
operated by
BATTELLE
for the
UNITED STATES DEPARTMENT OF ENERGY
Under Contract EY-76-C-06-1330

Printed in the United States of America
Available from
National Technical Information Service
United States Department of Commerce
5285 Port Royal Road
Springfield, Virginia 22151

Price: Printed Copy $____*; Microfiche $3.00

*Pages	NTIS Selling Price
001-025	$4.00
026-050	$4.50
051-075	$5.25
076-100	$6.00
101-125	$6.50
126-150	$7.25
151-175	$8.00
176-200	$9.00
201-225	$9.25
226-250	$9.50
251-275	$10.75
276-300	$11.00

PNL-2938
UC-79e

COBRA-IV WIRE WRAP DATA COMPARISONS

T. E. Donovan
T. L. George
C. L. Wheeler

February 1979

Prepared for
the U.S. Department of Energy
under Contract EY-76-C-06-1830

Pacific Northwest Laboratory
Richland, Washington 99352

CONTENTS

FIGURES

NOMENCLATURE

Arabic

A - area

C - concentration

D - rod diameter

D_h - hydraulic diameter

s - gap width

H - enthalpy

m - mass flow rate

P - pressure or pitch

Re - Reynolds number

$$\frac{\rho V D_h}{\mu}$$

t - wire wrap thickness

T - temperature

V_A - axial velocity

V_B - average axial velocity

V_T - transverse velocity

W - gap mass crossflow - $\frac{lb}{hr\text{-}ft}$

X - axial location (in. or cm)

Greek

δ - fraction of a wire wrap pitch over which cross-flow is forced

$\Delta( )$ - finite increment of ( ) (e.g., ΔX)

ϕ - angle between the tangent to the wire wrap and the axis of the encircled fuel rod

μ - viscosity

Superscript

$\overline{\quad}$ - average value

Subscripts

i - pertaining to subchannel i

j - pertaining to axial node j

k - pertaining to gap k

n - nominal value

o - pertaining to point of injection

in - inlet

out - outlet

COBRA-IV WIRE WRAP
DATA COMPARISONS

INTRODUCTION

Thermal hydraulic analyses of hexagonally packed wire-wrapped fuel assemblies are complicated by the induced crossflow between adjacent subchannels. Several computer codes[1] have been designed or modified to apply to wire-wrapped fuel assemblies. These codes can be categorized according to the manner in which the hydrodynamics are resolved. One category considers only the distribution of energy within a fuel assembly. This is accomplished by assuming that the flow variables (velocities and/or flow rates through subchannel and gap areas) are known (either empirically or by flow-split techniques). The second code category solves the fuel assembly hydrodynamics simultaneously with the thermodynamic calculation. Such a fundamental approach is desirable if calculations are necessary for a broad range of operating conditions.

The COBRA-IV computer code employs this fundamental approach to analyze the hydrodynamics and thermodynamics of fuel assemblies. A previous version of the COBRA code[2] incorporated a model to account for the presence of wire wraps in a fuel assembly. Basically, this model assumes that a forced crossflow (equal to a fraction of the axial flow rate) occurs near an axial location where a wire wrap enters the gap between fuel rods or a fuel rod and the assembly wall. Unforced crossflows (at the same axial location) are found by solving the transverse momentum equation. Some minor modifications were made to this model to improve the comparisons with available data.[1-6]

This report delineates the modifications and presents the results predicted by the COBRA-IV calculation and compares them with data measured in five experimental models of a wire-wrapped fuel assembly. The flow quantities compared are:

- subchannel salt concentrations/injection concentrations (C/C_o)
- axial and transverse velocities $\left(\frac{V_A}{V_B} \setminus \frac{V_T}{V_B}\right)$ in peripheral subchannels
- pressures and pressure differentials for various bundle flow rates.

The experimental results with which the COBRA-IV predictions are compared are the :

1.	ANL salt trace data	(91-pin bundle)[3]
2.	ANL dye trace data	(91-pin bundle)[1]
3.	MIT Laser-Doppler velocity measurement	(61-pin bundle)[4]
4.	French pressure data	(19-pin bundle)[6]
5.	ORNL heated data	(19-pin bundle)[5]

ANALYTICAL MODEL

The wire wrap model used for these data comparisons is essentially the same as that found in COBRA-IIIC. This model is discussed in detail in Reference 2, but will be briefly described in this section. Modification to the model are also documented in this section.

COBRA-IIIC WIRE WRAP MODEL

The model is based on assumption that the crossflow induced by the wire wrap passing through a gap is some fraction of the subchannel flow. The expression developed for the fractional split is

$$w_{forced} = \pi(D+t)\ (s/A_i)\ (\delta/\Delta x)m_i$$

where

- D is the rod diameter
- t is the wire wrap diameter
- S is the gap width
- A_i is the area of the subchannel contributing the forced crossflow
- m_i is the subchannel flow rate
- Δx is the axial node length
- δ is the arbitrary parameter, usually set to Δx/wire wrap pitch length.

Subchannel flow areas and wetted perimeters are adjusted to account for the presence of a wire wrap in the subchannel. The forced crossflows are then held constant while solving the transverse momentum equations for the remaining crossflows.

WIRE WRAP MODEL MODIFICATIONS

For these data comparisons, the wire wrap model was slightly modified to improve the results. The modifications include:

1. The reduction in the subchannel flow area due to the presence of a wire wrap is only half as large as the wire wrap cross sectional area, i.e.,

$$A_i = A_{i,n} - \frac{\pi(t/2)^2}{2}$$

where $A_{i,n}$ is the nominal subchannel area.

2. Use $\delta = 1.25\ \Delta x$/wire wrap pitch.

3. The method of solving the transverse and axial momentum equations requires keeping track of the pressure drop across each gap at each axial node. The pressure drop across a gap, k, at axial node, j-1, is given by

$$\Delta P_{k,j-1} = \Delta P_{k,j} - (dP/dx_{1,j} - dP/dx_{2,j})\Delta x$$

where $\Delta P_{k,j}$ is the pressure drop across a gap, k, at axial node j and dP/dx_i is the axial pressure drop for subchannel i. For gaps around the periphery of a bundle it was found helpful to calculate the transverse pressure drop according to:

$$\Delta P_{k,j-1} = \Delta P'_{k,j} - (dP/dx_{1,j} - dP/dx_{2,j})\Delta x$$

where

$$\Delta P'_{k,j} = 0.9\ \Delta P_{k,j} + 0.1\ \Delta P_F$$

where

$$\Delta P_F = \begin{cases} \text{a.)} \quad \Delta P_{k,j} \text{ if the gap is not forced.} \\ \text{b.)} \quad C_{k,j} W_{k,j} + \frac{\ell}{s} \frac{\tilde{U}_j W_{k,j} - \tilde{U}_{j-1} W_{k,j-1}}{x} \text{ if the gap is forced.} \end{cases}$$

This modification effectively transmits some of the pressure drop required for the forced crossflow to the nodes upstream of the forced gap.

The definitions and values of the crossflow resistance, $C_{k,j}$ and the ratio of the gap width to the inter-centroid distance s/ℓ, are given in Reference 7. Other COBRA parameters are set to the default values.

COMPARISON OF COBRA-IV TO EXPERIMENTAL DATA

In this section, the data available from the five experimental models is compared with the results computed from the COBRA-IV computer code. A brief explanation of the experimental apparatus, measured flow variable, and measurement technique is given for each experiment. Where necessary, a short description of the code modifications needed for the computer simulation is given.

ANL SALT TRACE DATA

Experiment

The ANL salt trace experiment[3] was performed in a model 91-pin fuel assembly (24 in. pitch) using water to simulate the coolant flow. A salt solution of a known concentration was injected at a measured flow rate into two peripheral subchannels diametrically opposed across the bundle. The total flow in various subchannels was extracted isokinetically at nine equidistant axial locations, the last of which was located 36 in. from the point of injection. The concentration of the extracted fluid was then determined by comparing its electrical conductivity to that of a solution of known concentration. These concentrations were then divided by the injection subchannel concentration to form a nondimensional concentration, C/C_o, which is plotted for the peripheral subchannels on Figure 1 and 2. The various experimental and theoretical curves correspond to different axial locations.

Computer Simulation

The COBRA program was used to simulate the salt injection experiment by recognizing the analogy between concentration and enthalpy:

$$C/C_o = \frac{H - H_{in}}{H_{out} - H_{in}} \qquad (1)$$

The enthalpy of the fuel assembly subchannel in program COBRA corresponding to that of the experimental injection subchannel was increased by an arbitrary

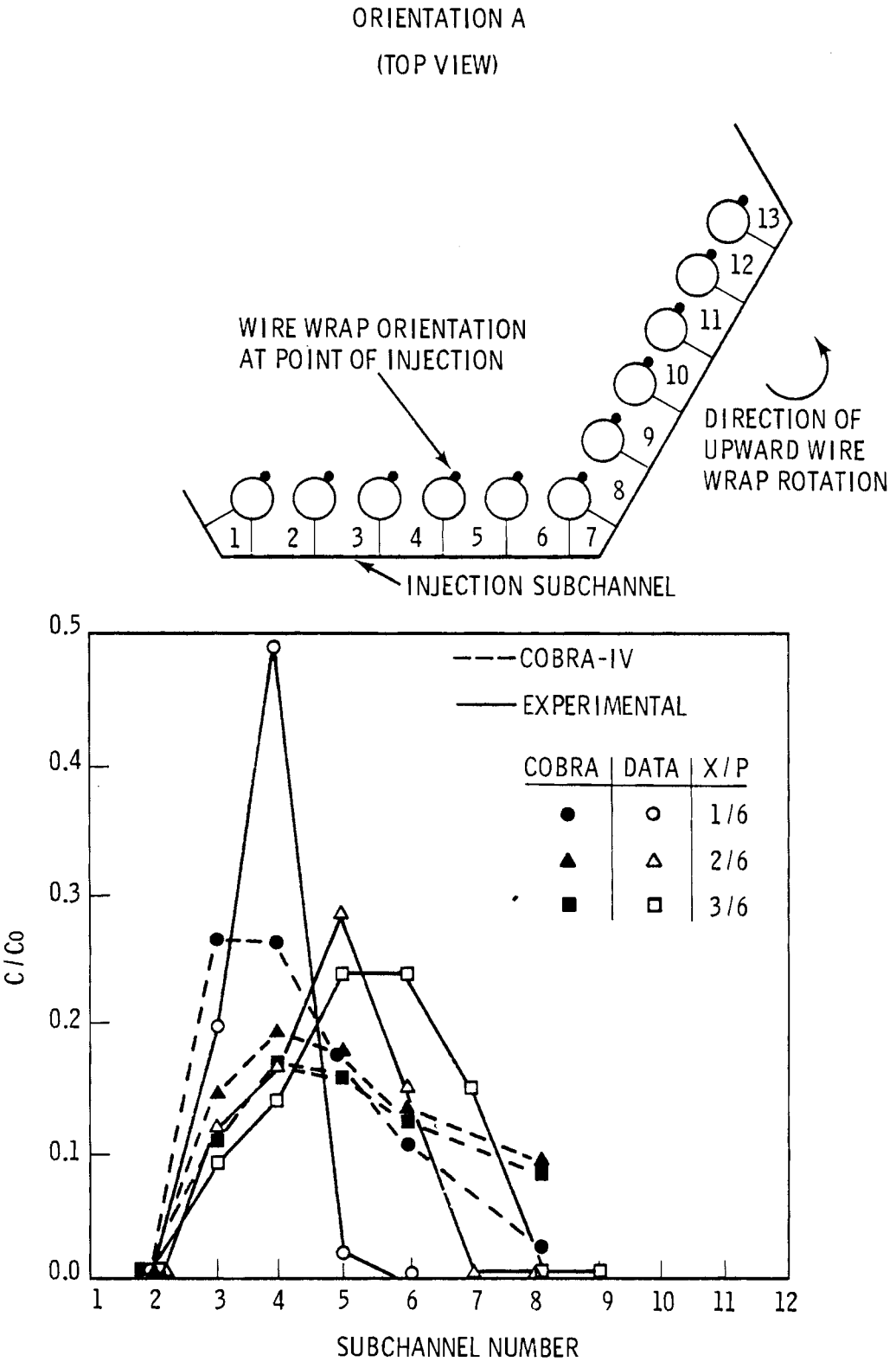

FIGURE 1. Subchannel Concentrations

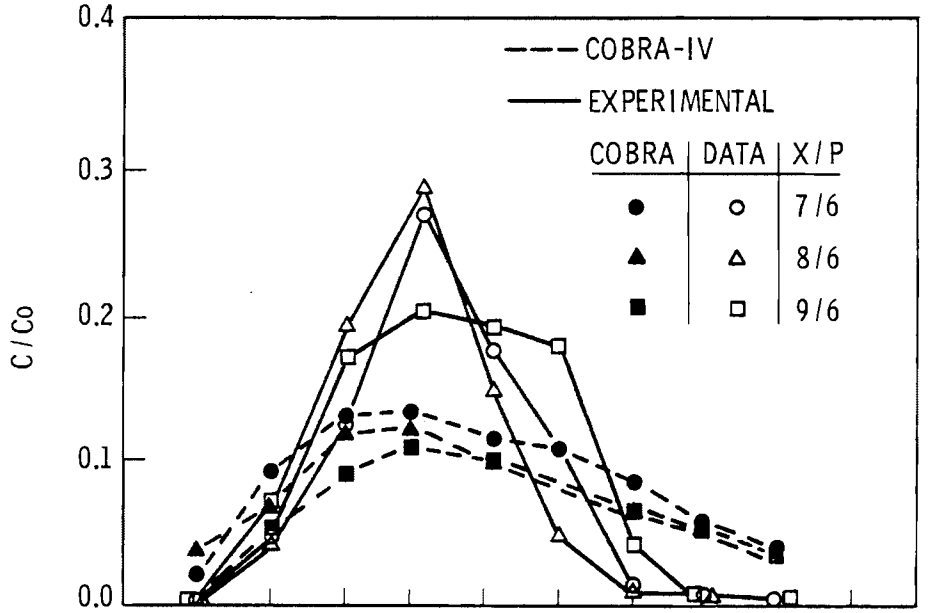

FIGURE 1b.

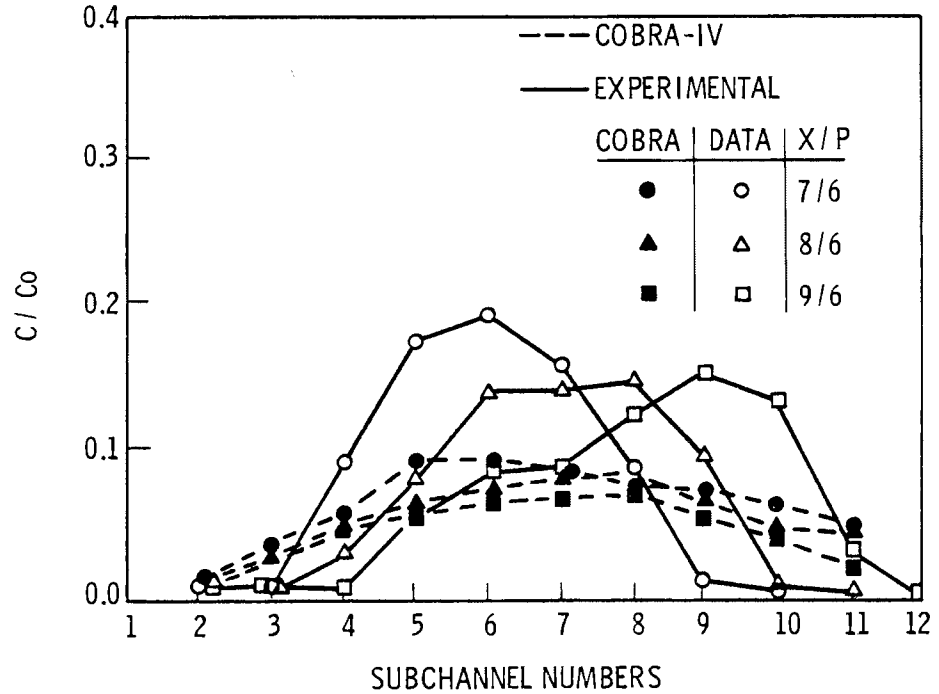

FIGURE 1c.

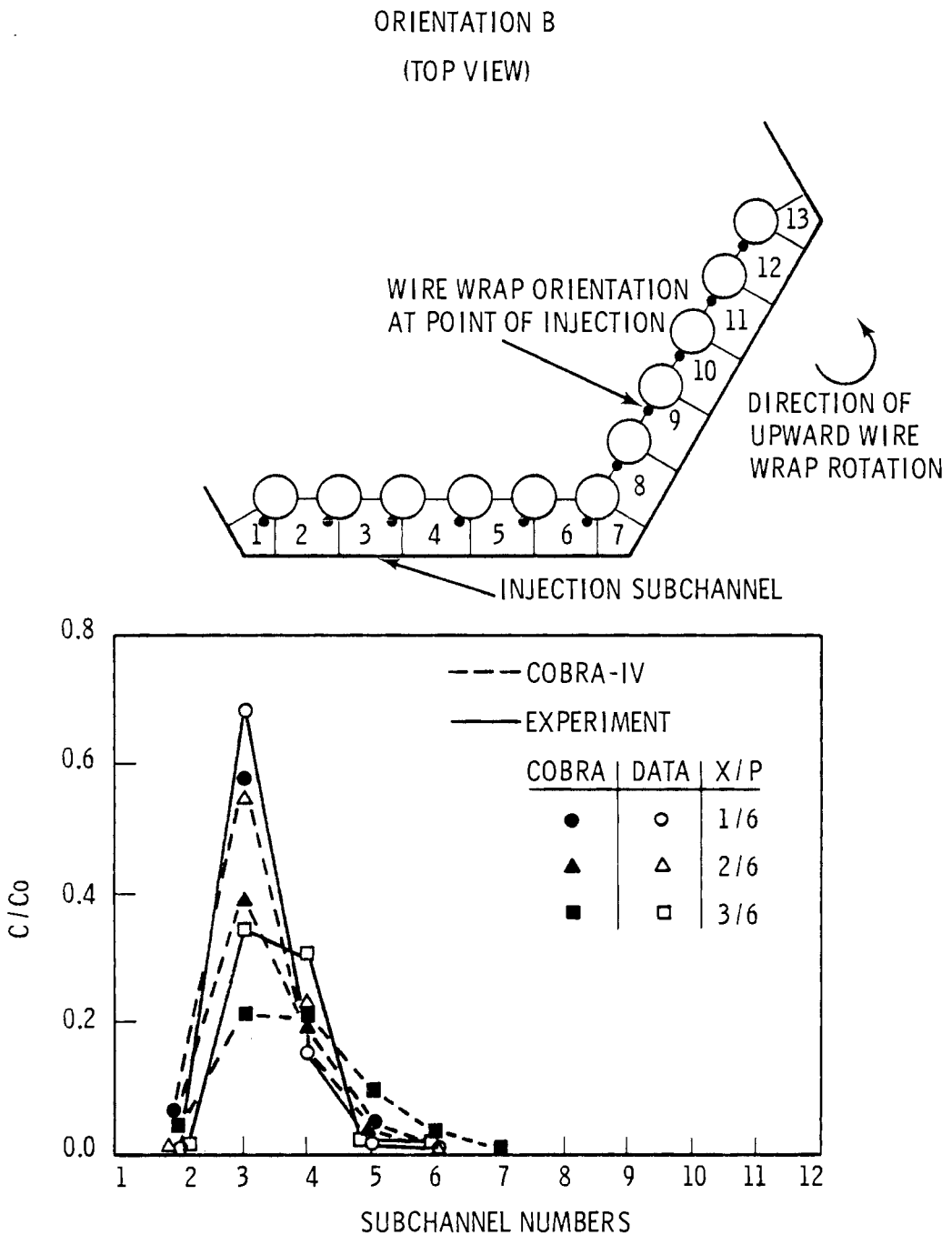

FIGURE 2. Subchannel Concentrations

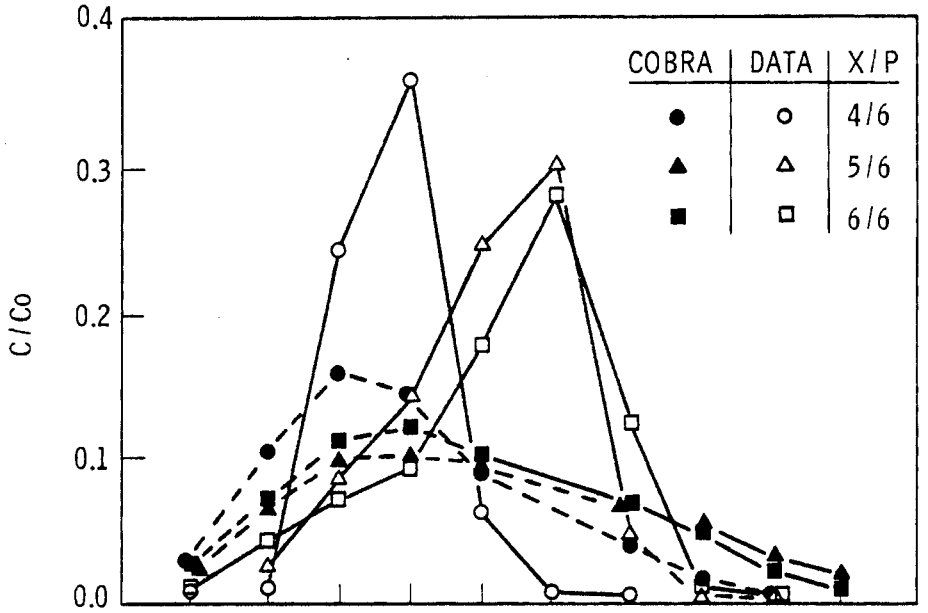

FIGURE 2b.

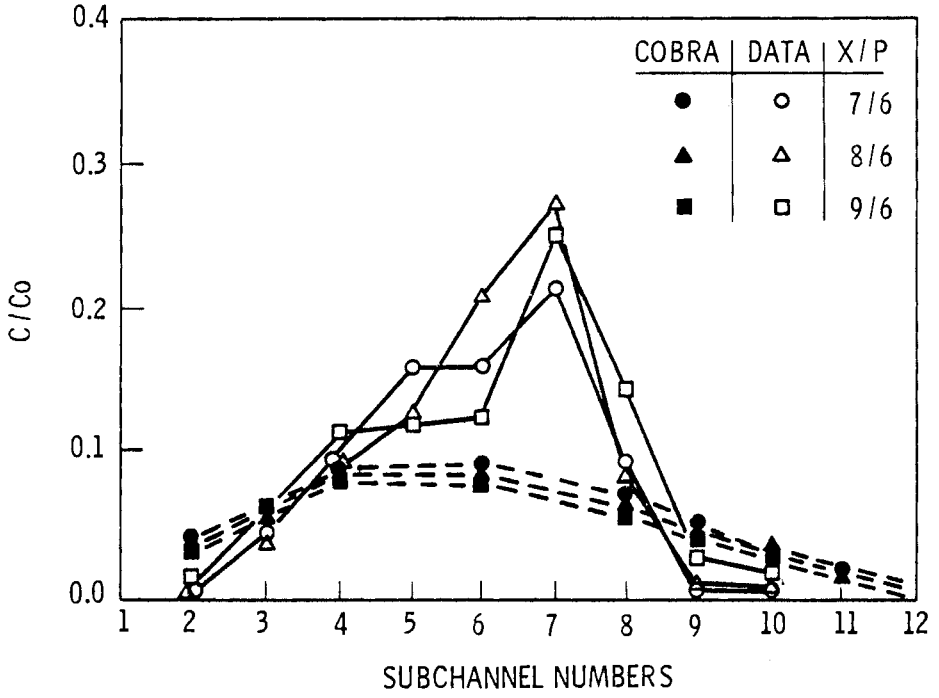

FIGURE 2c.

amount (50 Btu/lbm) over the nominal at an axial location one pitch length from the entrance (to minimize entrance effects). The nondimensional enthalpy ratio, given in Equation (1), was calculated for every peripheral subchannel and axial node. The results of these calculations are plotted in Figures 1 and 2 along with the experimental results.

Results and Discussion

Locus of Salt Concentration Maxima

The location of the maximum salt concentration (both experimental and theoretical) in the peripheral subchannels is shifted to the right (in the direction of the wire wrap induced crossflow) as the axial distance from the point of injection is increased. It can be seen from figures 1 and 2 that the results of the COBRA computer program are generally in agreement with the experimental salt concentration maxima. Because the locus of this maximum corresponds to the flow direction in the peripheral subchannels, the agreement of the theory with the experiment is a partial confirmation of the code's hydrodynamic solution.

Concentration Diffusion

Comparison of the experimental data with the results of the COBRA computation show that the theoretical salt concentration profiles tend to spread faster than in the experimental apparatus. This is evidenced by the fact that the theoretical profiles are smaller in magnitude than the experimental profiles in the region of the concentration maximum. Further, the theoretical profiles have a larger "tail" in the direction of the wire wrap induced crossflow. Because turbulent mixing was not allowed in these calculations, this flattening effect is attributed to the numerical diffusion inherent to the upwind enthalpy advection scheme utilized by the code.

ANL DYE TRACE DATA

Experiment

The ANL dye trace experiment[1] is geometrically similar to the ANL salt trace data except for a relatively minor difference in the bundle pitch ratio (P/D). However, an opaque dye was injected in a peripheral subchannel

(corresponding to injection orientation A in the salt trace experiment) and its subsequent movement was observed visually through a plexiglass wall forming half of the bundle enclosure.

Results and Discussion

The path of the experimental dye concentration maxima is given on Figure 3. Because the COBRA computer code calculates average values of subchannel enthalpy for each axial increment, the computational results are presented by outlining the subchannel segment containing the maximum enthalpy (i.e., dye concentration) at every axial location. The agreement between the experimental locus of maximum dye concentration and that resulting from the COBRA numerical calculation is good. This is to be expected because, as shown in the previous section, the COBRA code successfully predicted the path of the maximum salt concentration through the bundle in the ANL salt trace experiment.

MIT LASER-DOPPLER VELOCITY MEASUREMENTS

Experiment

Axial and transverse velocity measurements were made in the peripheral subchannels of a simulated 61-pin fuel assembly.[4] These measurements were obtained using a laser-Doppler system operating in the backscattering mode.

The test bundle consists of 61 wire-wrapped rods, 0.25 in. in diameter and 50 in. long. They are arranged in a triangular pitch with a separation distance of 0.0625 in. (the wire wrap diameter). Wire wrap pitches of 6 and 12 in. were used in these experiments.

Data obtained in this experiment is presented as a ratio of the transverse velocity to the nominal bundle velocity, V_T/V_B. The nominal bundle velocity is calculated by using the measured experimental flow rate, m, the nominal bundle area, A_n, as:

$$V_B = \dot{m}/\rho A_n \qquad (2)$$

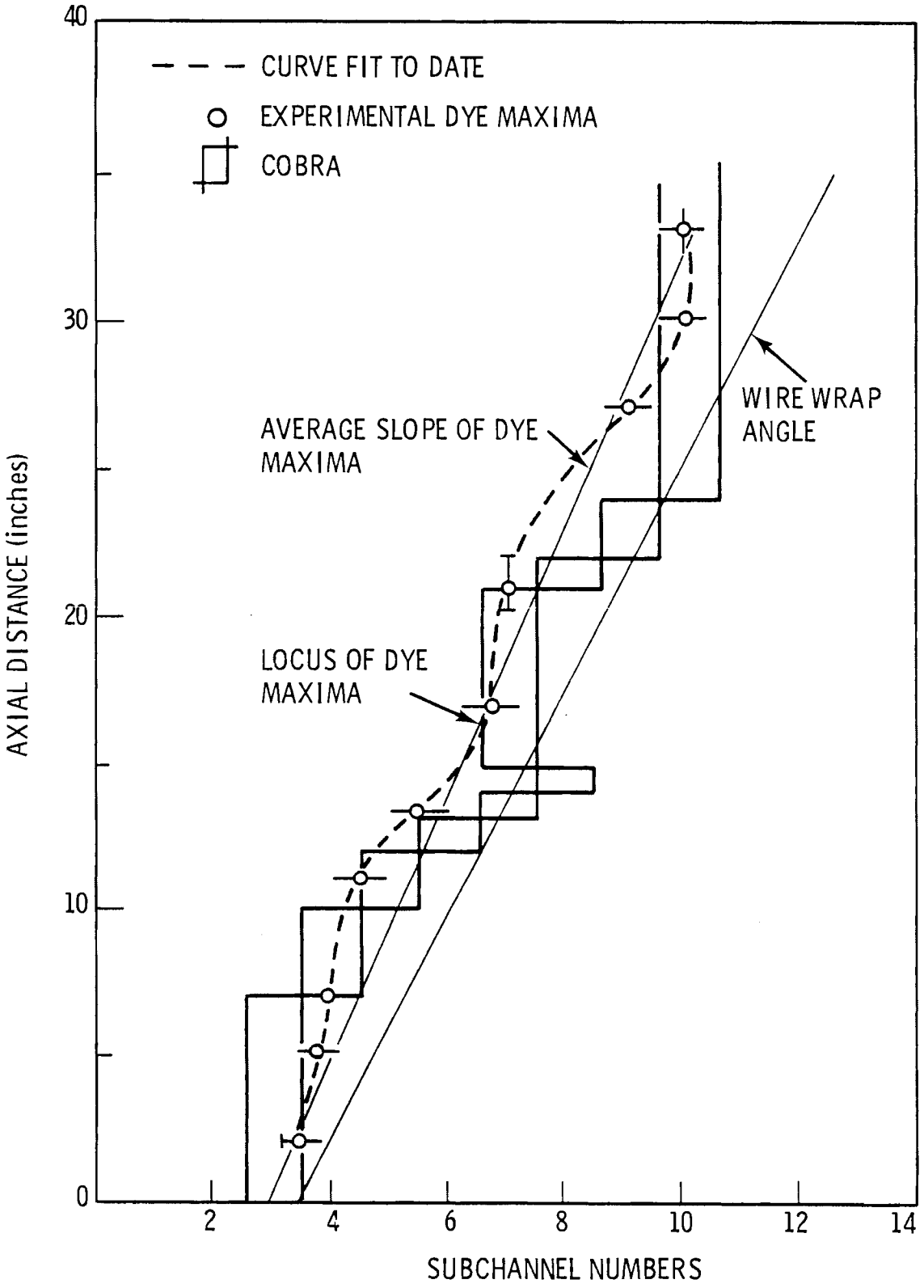

FIGURE 3. Path of Dye Concentration Maxima

The resulting nondimensional velocities are plotted as functions of axial distance for various transverse locations on the bundle periphery.

Computer Simulation

To correctly simulate the MIT experiment, the COBRA code was modified to output the nondimensional transverse velocity, V_T/V_B, in the peripheral gaps (between the rods and the bundle wall). This was calculated in terms of the gap crossflows, $W_{i,j}$ and gap width, s_i, (the i refers to the particular gap in question while j is the index of the axial location), according to:

$$\frac{V_T}{V_B} = \frac{W_{i,j}/\rho s_i}{V_B} \tag{3}$$

where V_B has been obtained from Equation (2).

Results and Discussion

The results of the experiment and the COBRA computation for a typical peripheral gap are presented in Figures 4 and 5 for two different wire wrap pitches. The agreement is seen to be best in the region farthest from the bundle inlet, x = o. This implies that entrance length effects may persist farther from the entrance than predicted by the COBRA code.

FRENCH PRESSURE DROP EXPERIMENT

Experiment

Measurements of the static pressure were made in various peripheral subchannels of a simulated 19-pin wire wrap fuel assembly in which water was used to simulate the coolant. These experiments were performed using as many as 11 different bundle mass flow rates. The resulting pressures were presented as a function of axial distance from inlet on an absolute basis in Figure 6 and on a relative basis (i.e., as a difference in pressures between a peripheral subchannel and the bundle average at an axial location) in Figure 7.

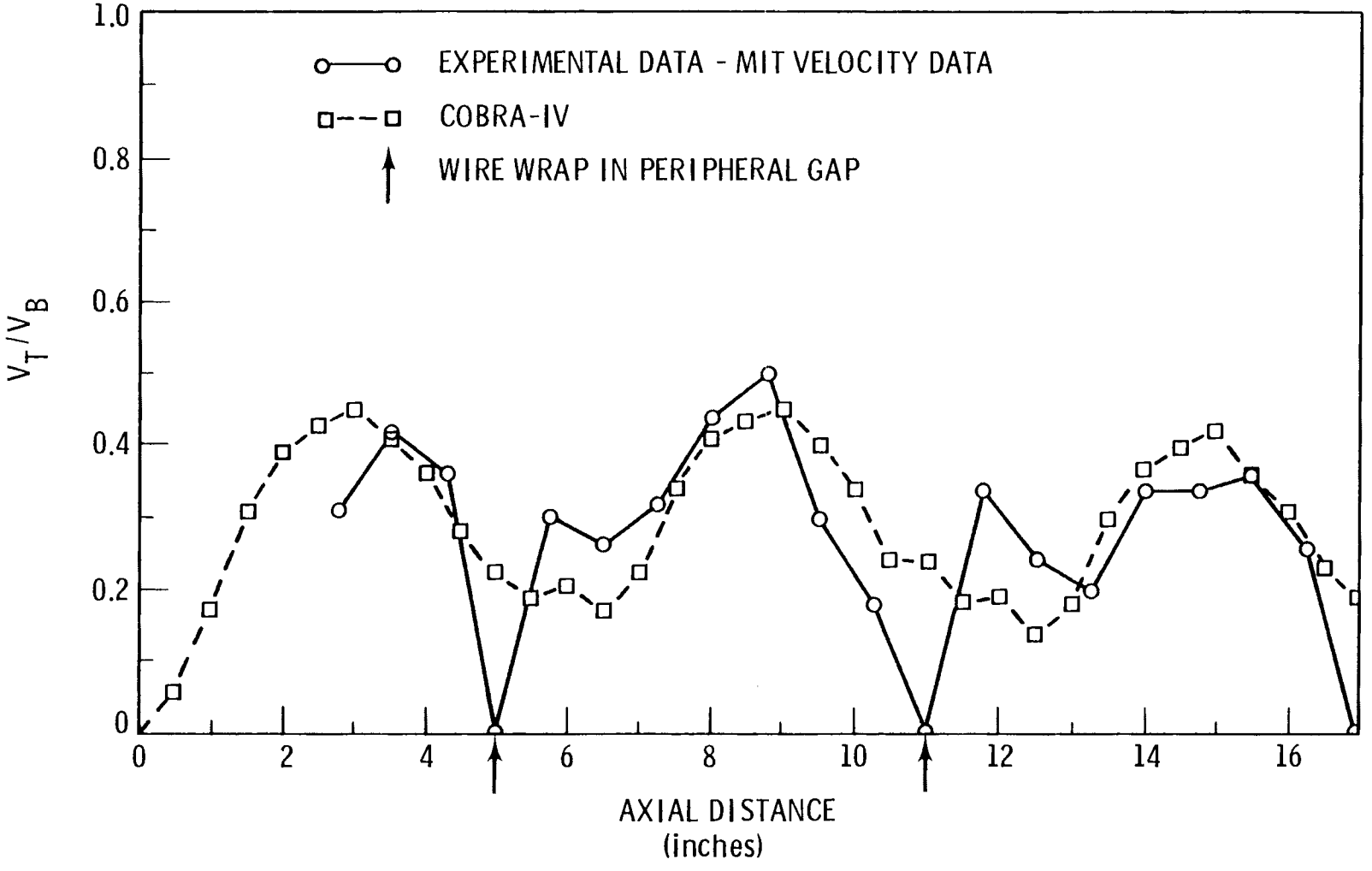

FIGURE 4. Nondimensional Crossflows (6 in. pitch)

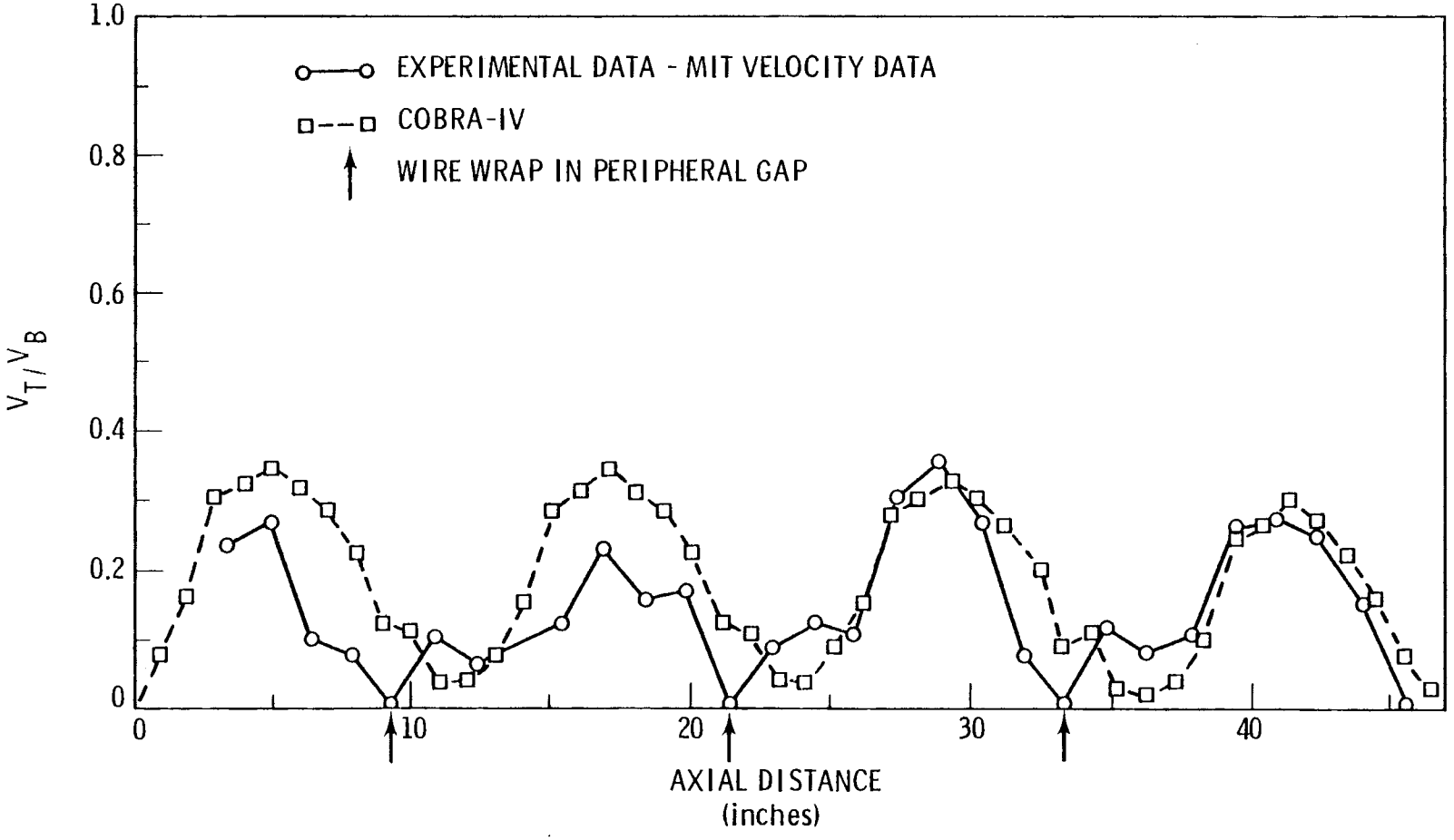

FIGURE 5. Nondimensional Crossflows (12 in. pitch)

Computer Simulation

Because the static pressure is a dependent variable of the COBRA solution algorithm, no code modification was necessary to simulate the experiment. The static pressure of a given subchannel for each axial node was obtained directly from the program output. Bundle mass flow rates (in M-lbm/hr-ft^2 of water), corresponding to those used in the experimental apparatus, were the only inputs (other than the inlet temperature and system pressure) necessary to model the experimental system.

The total theoretical pressure drop through the test bundle depended upon the friction factor employed by the code to calculate the subchannel flow resistance. Novendstern[7] obtained an expression that modifies the standard Fanning friction factor to include the effect of the wire wrap on the pressure drop through a wire-wrapped bundle. This friction factor is given as

$$f = 0.316\ M(Re)^{-0.25} \qquad (4)$$

where M is a function of the bundle pitch, the wire wrap pitch and the bundle Reynolds number (Re).

In this set of experiments, the largest value of M (corresponding to the largest bundle mass flow rate) was 1.3. Thus the flow resistance of the bundle is 30% above that of a bundle containing no wire wrap. The value of the multiplier, M, was calculated for each bundle mass flow rate used in the experiment. This value was used by the code in the friction factor calculation according to Equation (4).

Results and Discussion

The experimental axial static pressure distribution in a peripheral subchannel is given in Figure 6 for two different bundle mass flow rates. Also given are those predicted by the COBRA code for two of the mass flow rates. It can be seen that the COBRA results and the experimental values are in excellent agreement. That the code predicts the cyclic pressure behavior (whose period is equal to that of the wire wrap pitch) is of special interest. Also of special interest is the fact that the use of the "wire

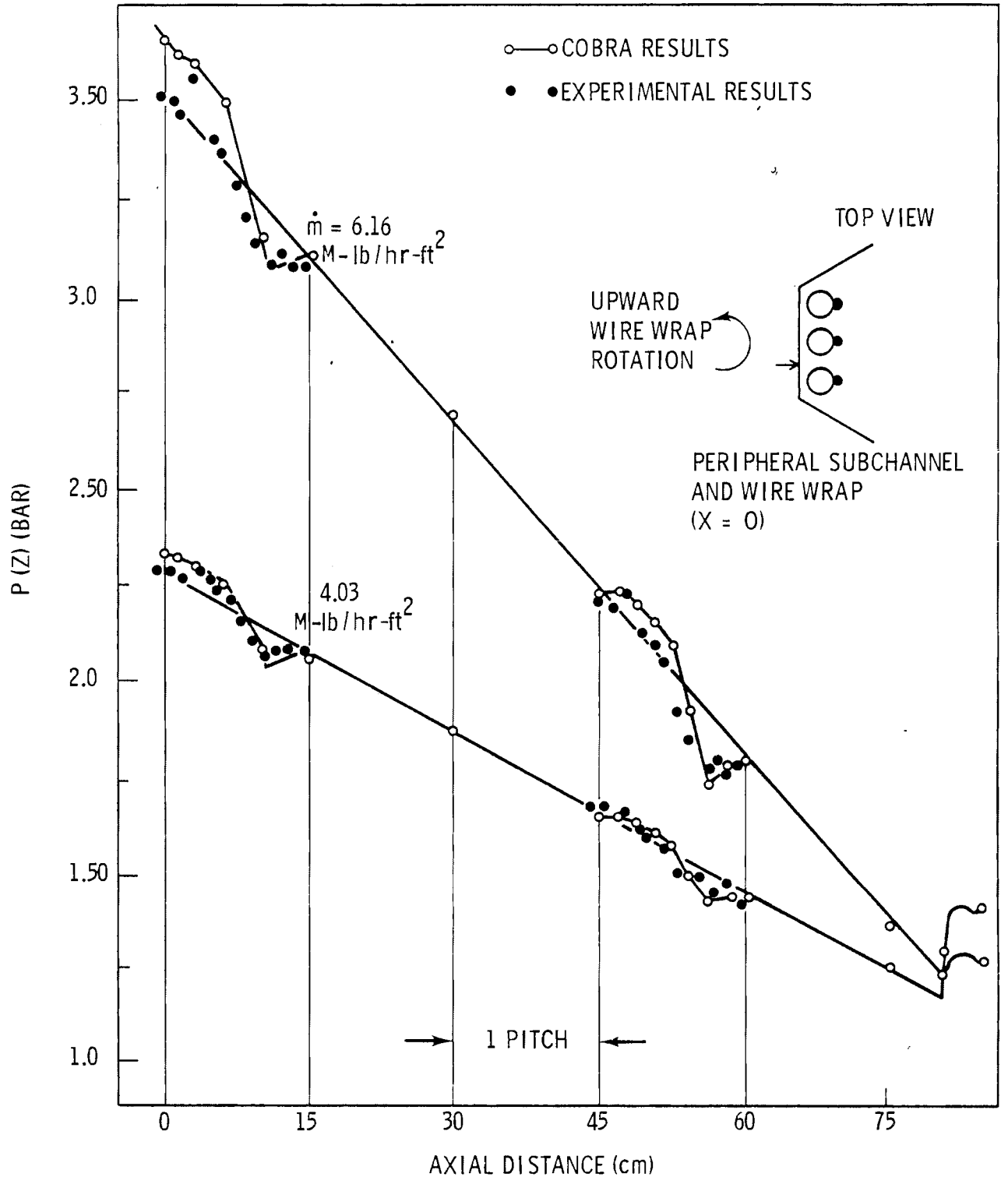

FIGURE 6. Axial Static Pressure in a Peripheral Subchannel

wrapped" friction factor, Equation (4) in the COBRA calculation yields excellent agreement with the experimental average pressure drop, drawn as solid lines on Figure 6.

The cyclic static pressure variation in a peripheral subchannel was examined more closely by forming the difference between the static pressure in a single peripheral subchannel and the average pressure of all peripheral subchannels at an axial location, x, according to

$$P(x) - \overline{P}(x) \tag{5}$$

This difference was calculated from experimental data taken over an axial distance equal to one wire wrap pitch and is shown in Figure 7. Figure 7 also shows the results of the COBRA calculation for two of the experimental flow rates. Again, the COBRA code predicted both the magnitude of the pressure difference and the correct periodic behavior of this quantity. Thus, the ability of the COBRA code to predict pressure fluctuations in wire wrapped fuel assemblies is clearly demonstrated.

ORNL HEATED BUNDLE EXPERIMENT

Experiment

The ORNL experiment was conducted with an electrically heated 19-pin wire-wrapped fuel assembly. The power output could be set independently for each pin. Varying the sodium coolant flow rate and the power distribution in the bundle made it possible to simulate a wide range of operating conditions (power skews, loss of pumping power, etc). Ungrounded thermocouples were located in the duct wall at various distances from the start of the electrically heated sections of the pins. Grounded thermocouples, located in a "rake", were positioned so that the temperatures of selected interior and peripheral subchannels could be measured at the bundle exit, 21 in. from the start of the electrically heated pins. Insulation was applied to the exterior of the bundle in an attempt to minimize radial heat losses.

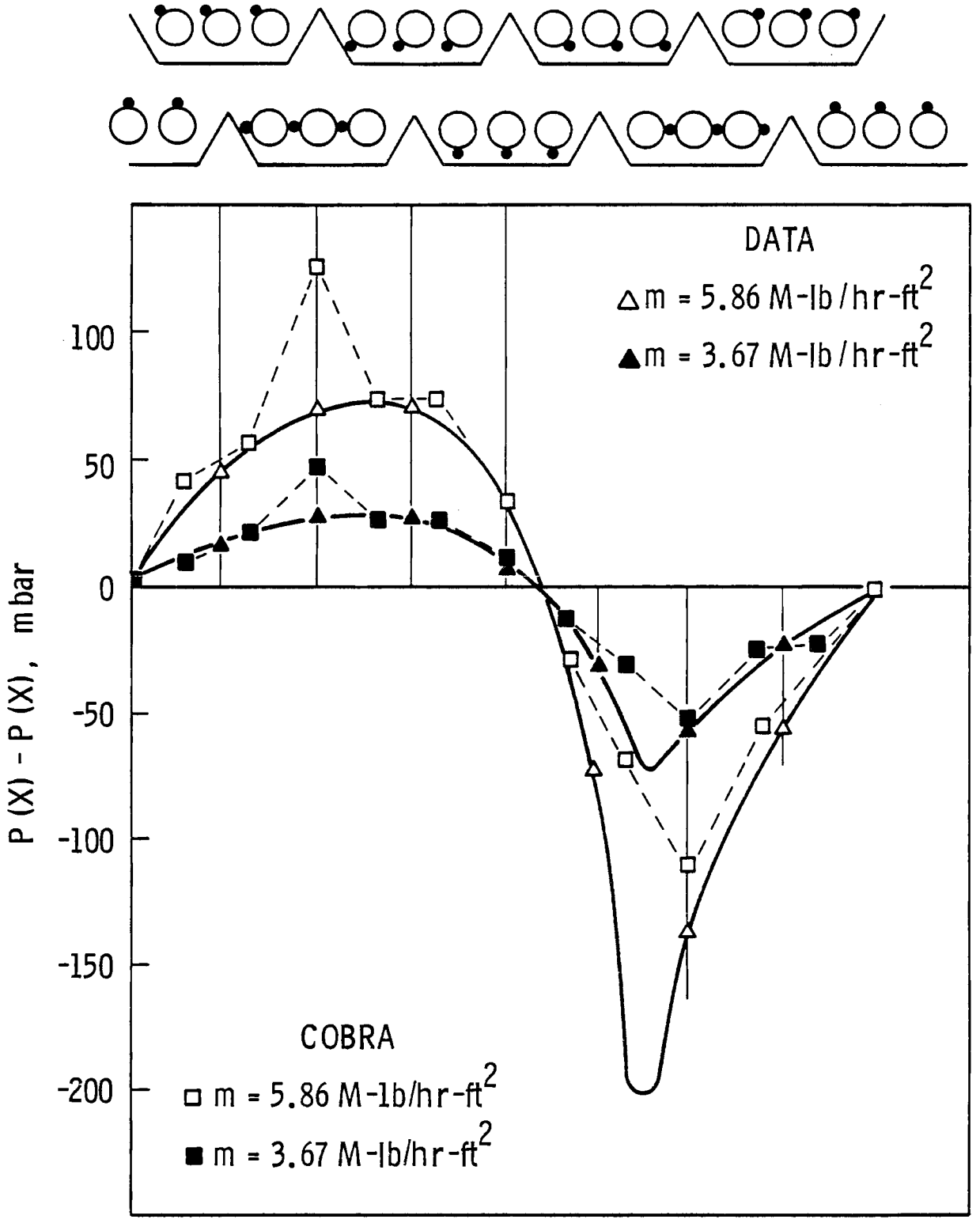

FIGURE 7. Cyclic Pressure Variation in a Peripheral Subchannel

The experimental bundle was operated for a wide range of coolant flow rates and electrical heating configurations. Two available[5] test cases were chosen for computer simulation:

1. Nominal power generation (5 kW/ft/rod) and mass flow rate (53 gpm of sodium).
2. Three peripheral rods (adjacent to the same duct flat) electrically heated (10 kW/ft/hr) and a nominal mass flow rate (54 gpm of sodium).

The first case is most representative or normal LMFBR operation while the second case provides a good standard for testing models for the lateral transport of energy in a bundle periphery. It should be noted that a total of six heating configurations (one for each flat) are possible for the three heated rod experiments.

The experimental temperatures (measured in the duct wall and in the interior subchannels 18 in. and 21 in. from the bundle inlet) were nondimensionalized according to

$$\frac{T - T_{in}}{T_{out} - T_{in}}$$

where T_{in} is the bundle inlet temperature and T_{out} is the average bundle outlet temperature. These nondimensional temperatures are shown (for various interior subchannels and duct wall locations) in Figures 8 and 9. The bundle positions of these subchannels and wall locations are shown in Figure 10.

Computer Simulation

The simulation of the experiment using the COBRA computer code is straightforward because the coolant flow rate and the power generation of each pin are set as standard input variables in the code. The input parameters for the two sets of data (nominal power generation case and the three heated pin experiments) are given below.

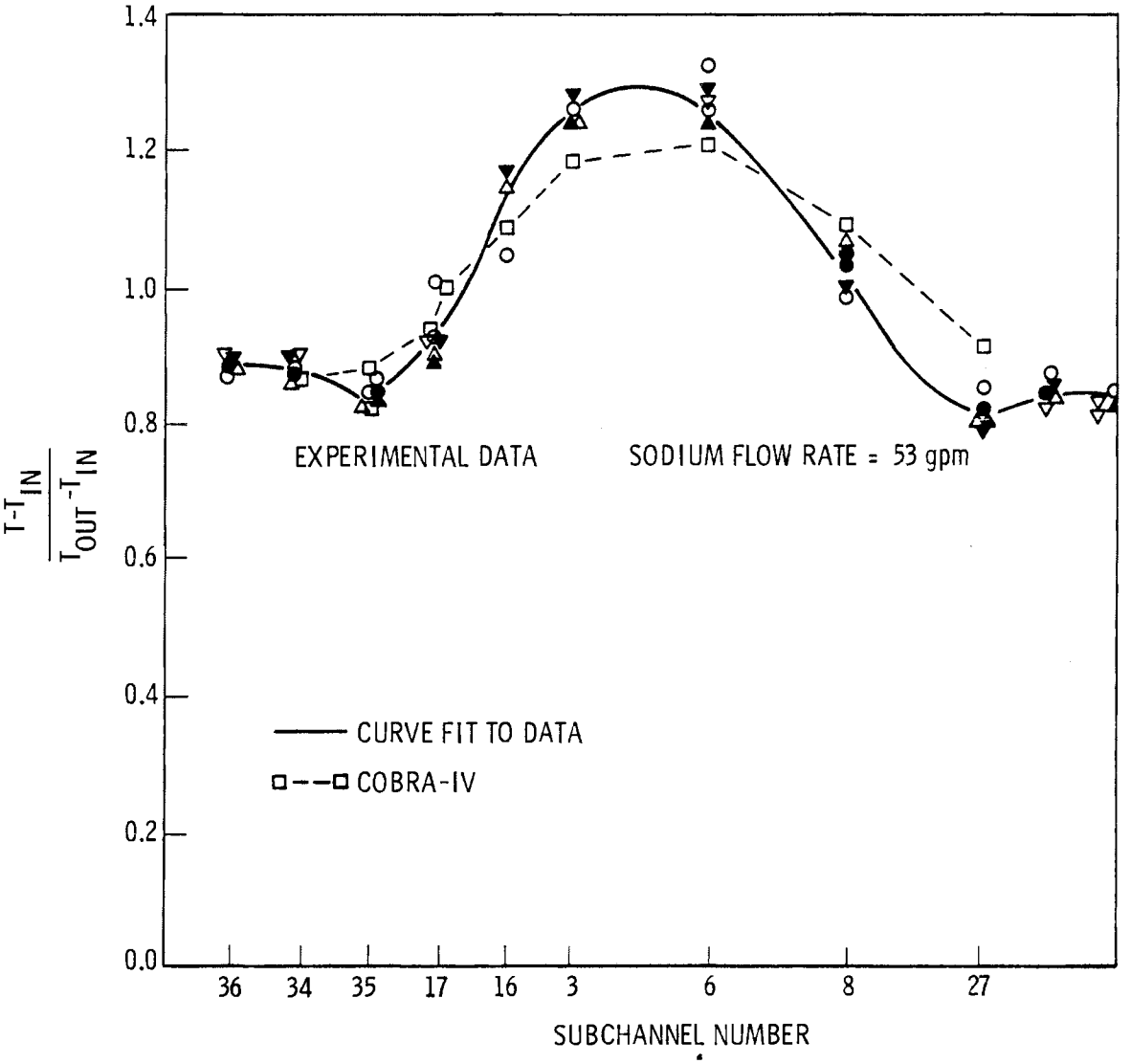

FIGURE 8. Bundle Exit Temperatures (X = 21 in.)

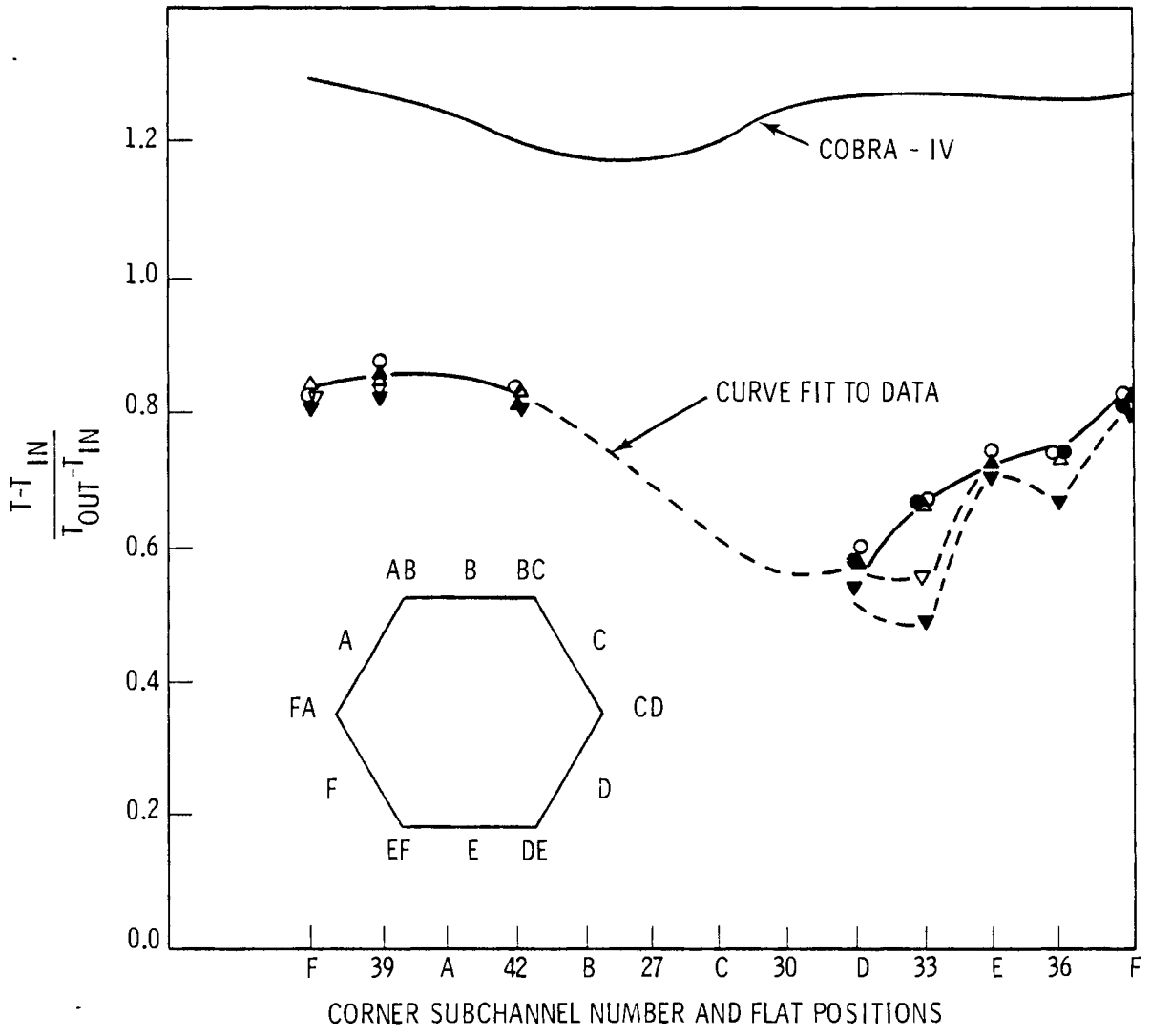

FIGURE 9. Duct Wall Temperature (X = 18 in.)

TABLE 1. Computer Simulation Input Parameters

	Power Generation	Coolant Flow Rate (gpm)
Nominal Operating Conditions	all rods-5 kW/hr/ft	53
3 Heated Pin Experiments	rods 16, 17, 18--10 kW/ft/hr	54
	rods 18, 19, 8--10 kW/ft/hr	54
	rods 14, 15, 16--10 kW/ft/hr	54
	rods 8, 9, 10--10 kW/ft/hr	54
	rods 12, 13, 14--10 kW/ft/hr	54
	rods 10, 11, 12--10 kW/ft/hr	54

The location of the rods is available on Figure 10. The nondimensional temperature was calculated according to

$$\frac{H - H_{in}}{H_{out} - H_{in}}$$

where the inlet enthalpy of the sodium coolant was evaluated at 600°F.

Results and Discussion

The outcomes of both computer simulations are described in the following paragraphs.

Nominal Operating Conditions

The nondimensional temperature profiles obtained at the exit of the heated bundle (x = 21 in.) for the normal operation of the bundle are given in Figure 8. COBRA code agreement with the experimental results is good. However, the location of the maximum temperature predicted by COBRA (subchannel 6) is clearly on the side of the fuel assembly toward flat B while the experimental profile is almost symmetric.

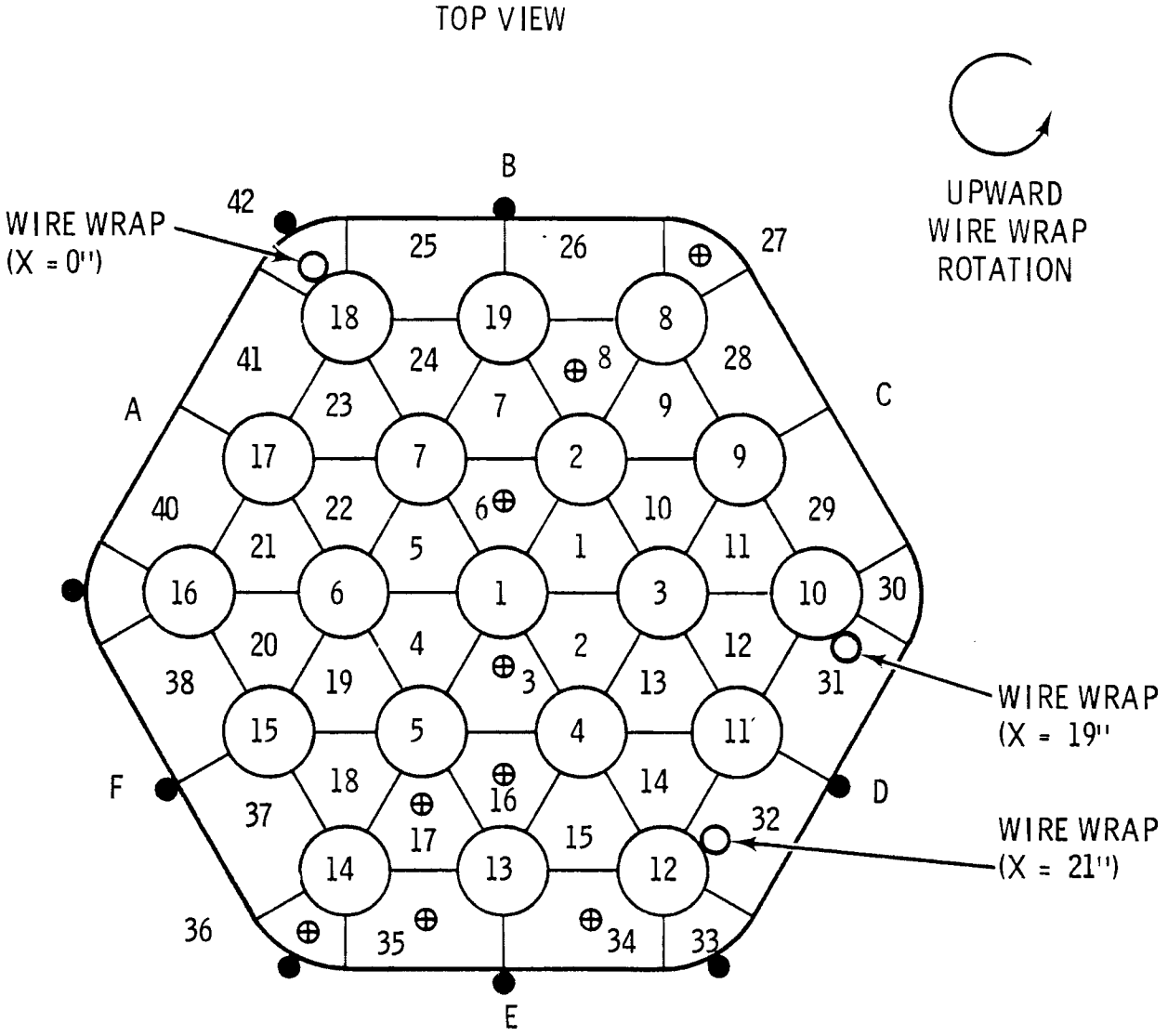

FIGURE 10. Rod and Subchannel Locations

The nondimensional temperatures measured on the duct walls 18 in. from the start along with the results of the COBRA calculation. The two results differ in both magnitude and phase. Similar results, obtained by ORNL, were believed to be caused by steep temperature gradients in the peripheral subchannels and bundle distortion. Changes in the ORNL analytical model to allow for this bundle distortion improved the phase agreement between the experimental and analytical results.

Three Heated Pins

The nondimensional temperatures resulting from the three heated pin experiments are shown in Figures 11 through 16 along with the analytical predictions resulting from COBRA calculations. Each figure also shows the locations of the three heated pins and the wire wrap position 18 in. from the start of the heated length. The theoretical predictions for all six experiments are similar in form. The location of the maximum temperature is always clockwise (to the right on the figures) of the central heated pin. The physical reason for this is that the wire wrap induced crossflow advects the energy released from the heated pins in this direction. Thus the location of the temperature maximum may be shifted some distance in the direction of flow. It can be seen that the agreement between theory and experiment is best when the wire wrap is on the far side of the pin (away from the periphery) and worst when it is fully in the peripheral gap. The exact reason for this disagreement is unknown, but it is thought to be caused by the previously mentioned bundle distortion or malfunctioning thermocouples in the duct wall.

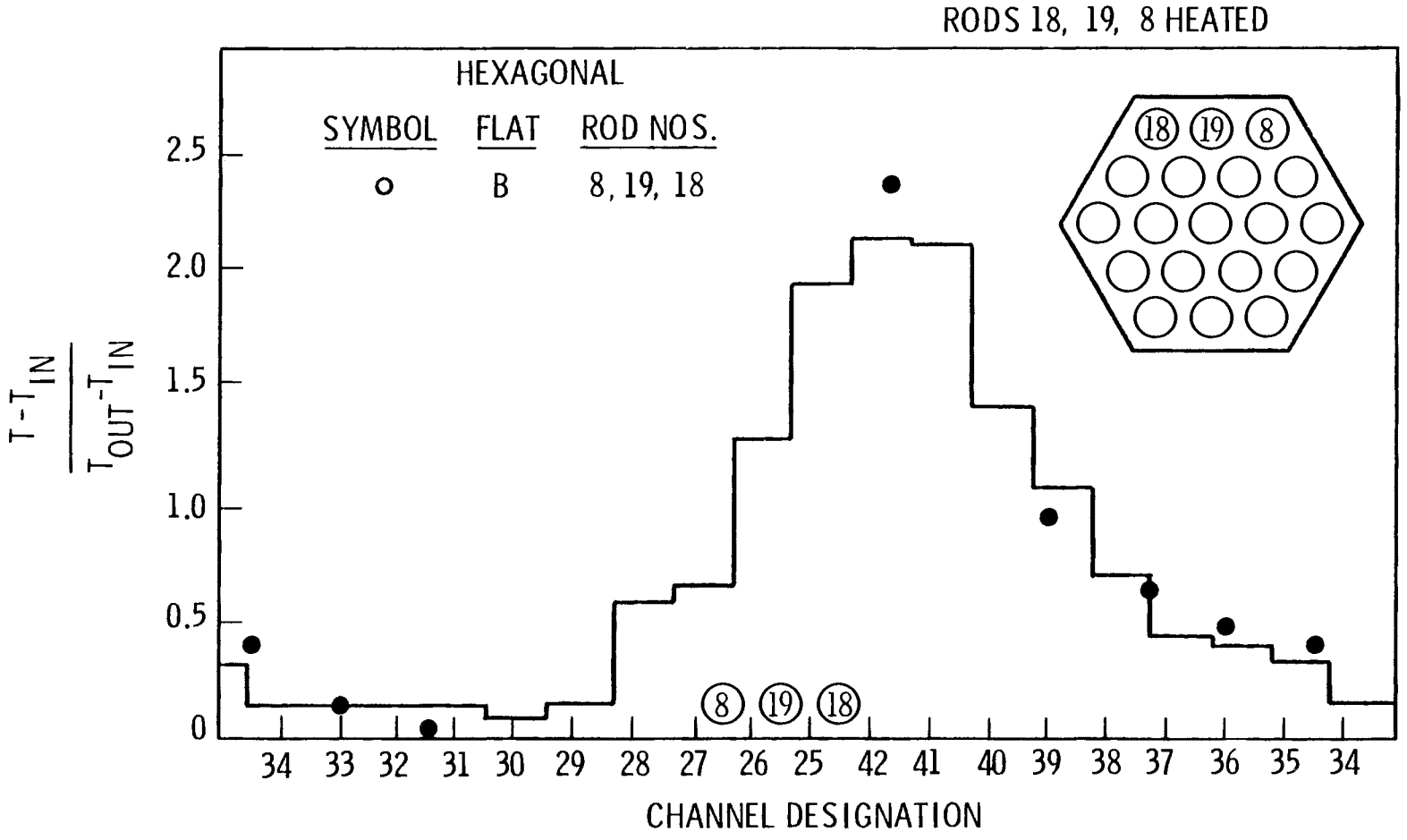

FIGURE 11. Peripheral Subchannel Temperatures (X = 18 in.)

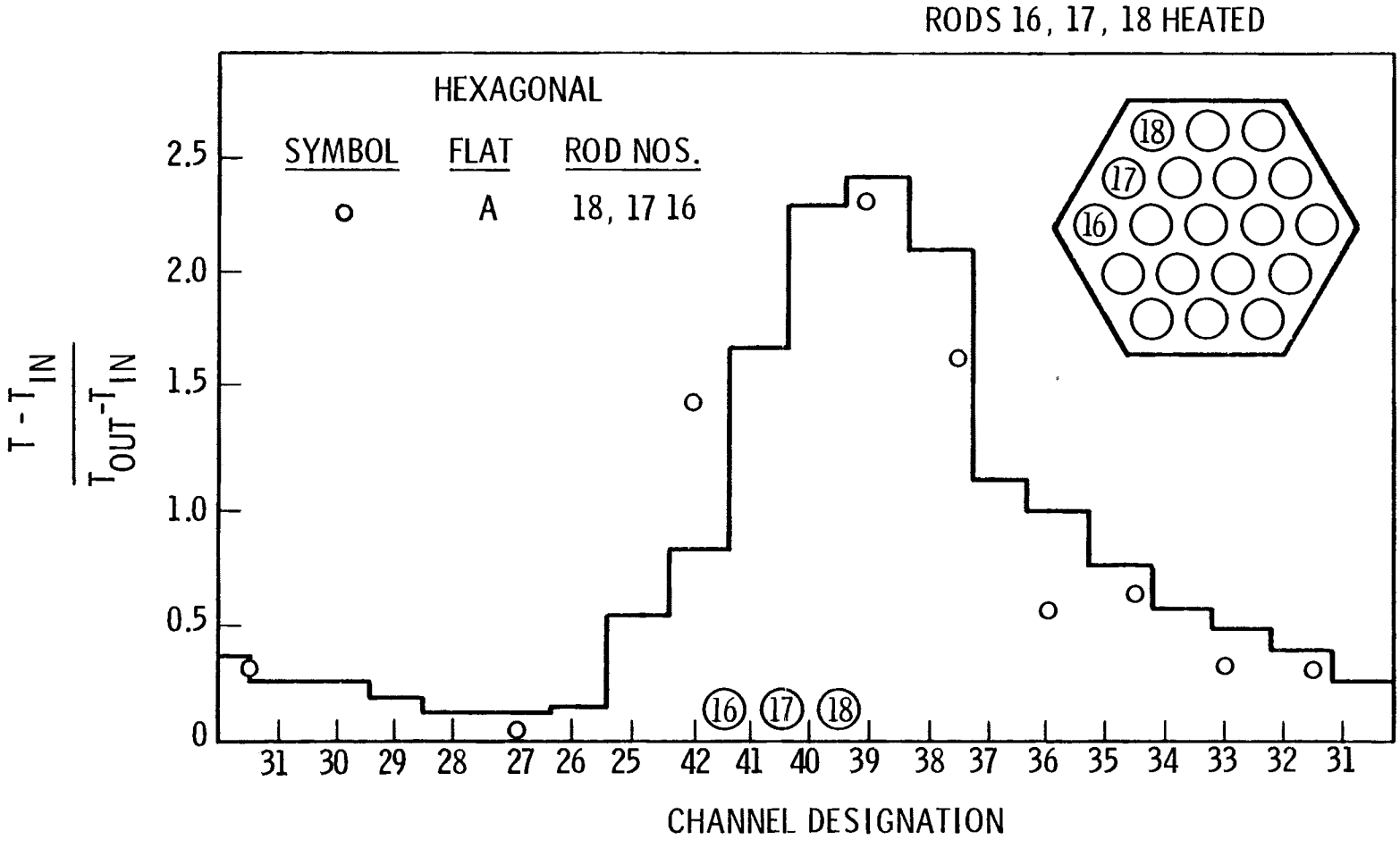

FIGURE 12. Peripheral Subchannel Temperatures (X = 18 in.)

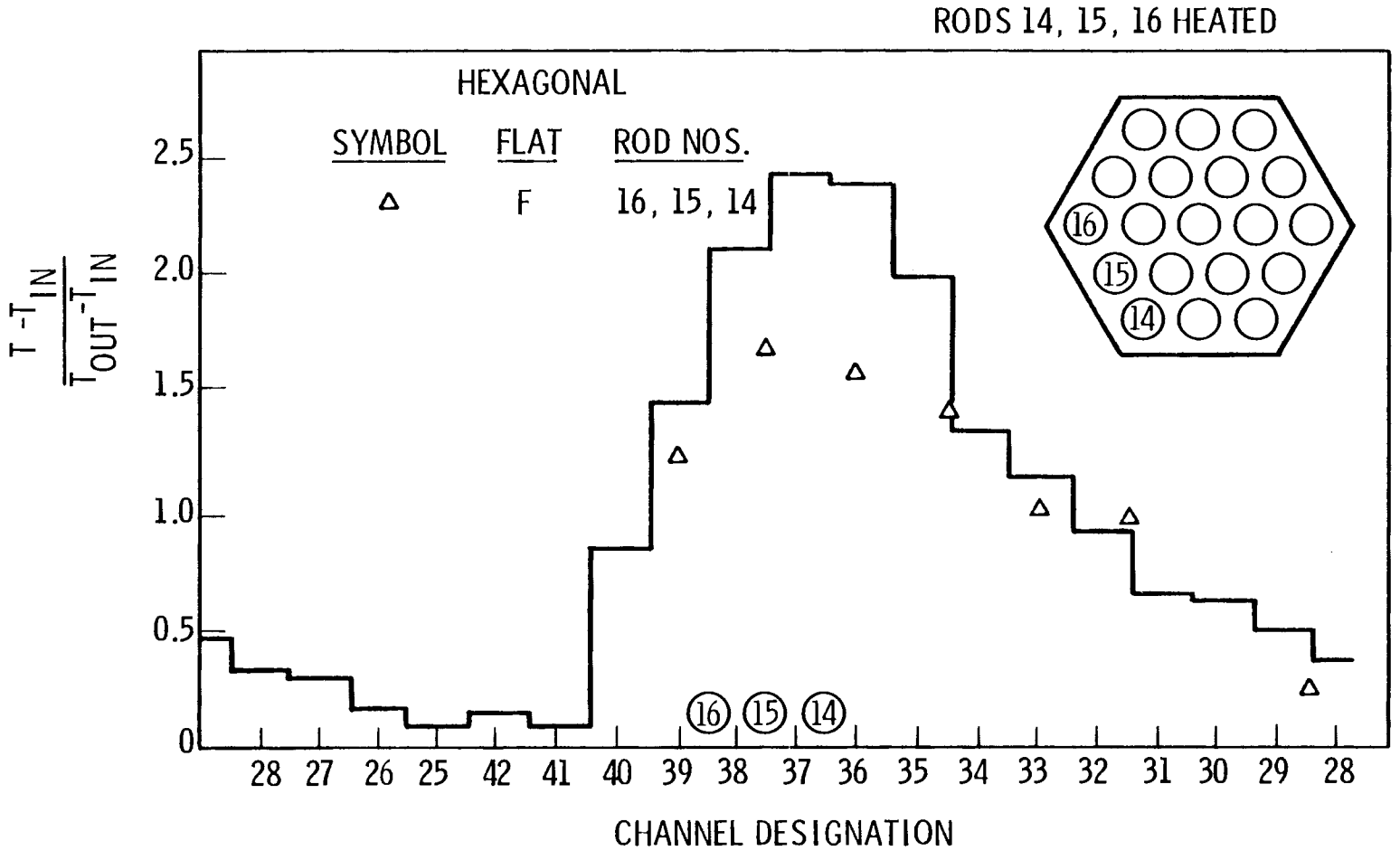

FIGURE 13. Peripheral Subchannel Temperatures (X = 18 in.)

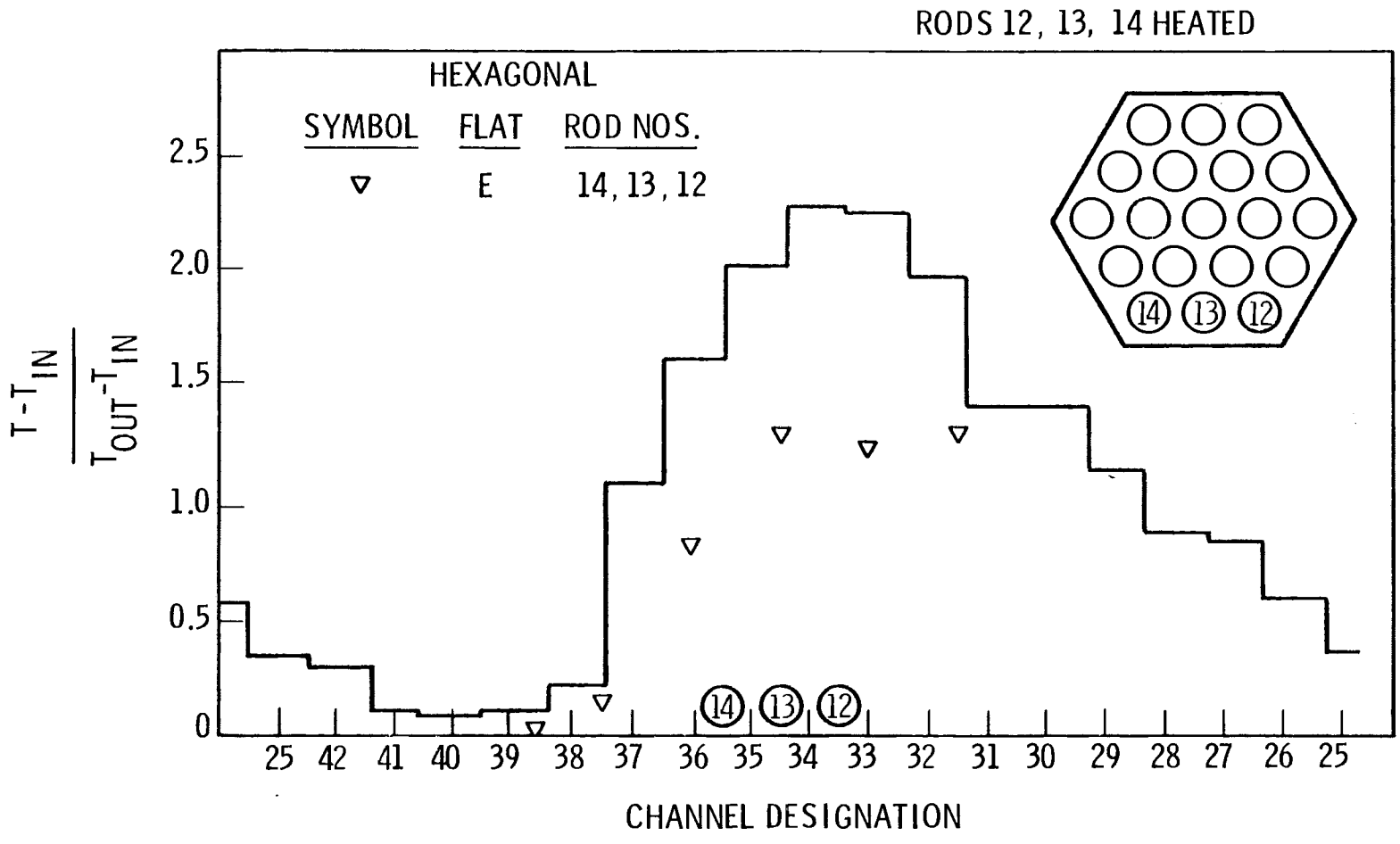

FIGURE 14. Peripheral Subchannel Temperatures (X = 18 in.)

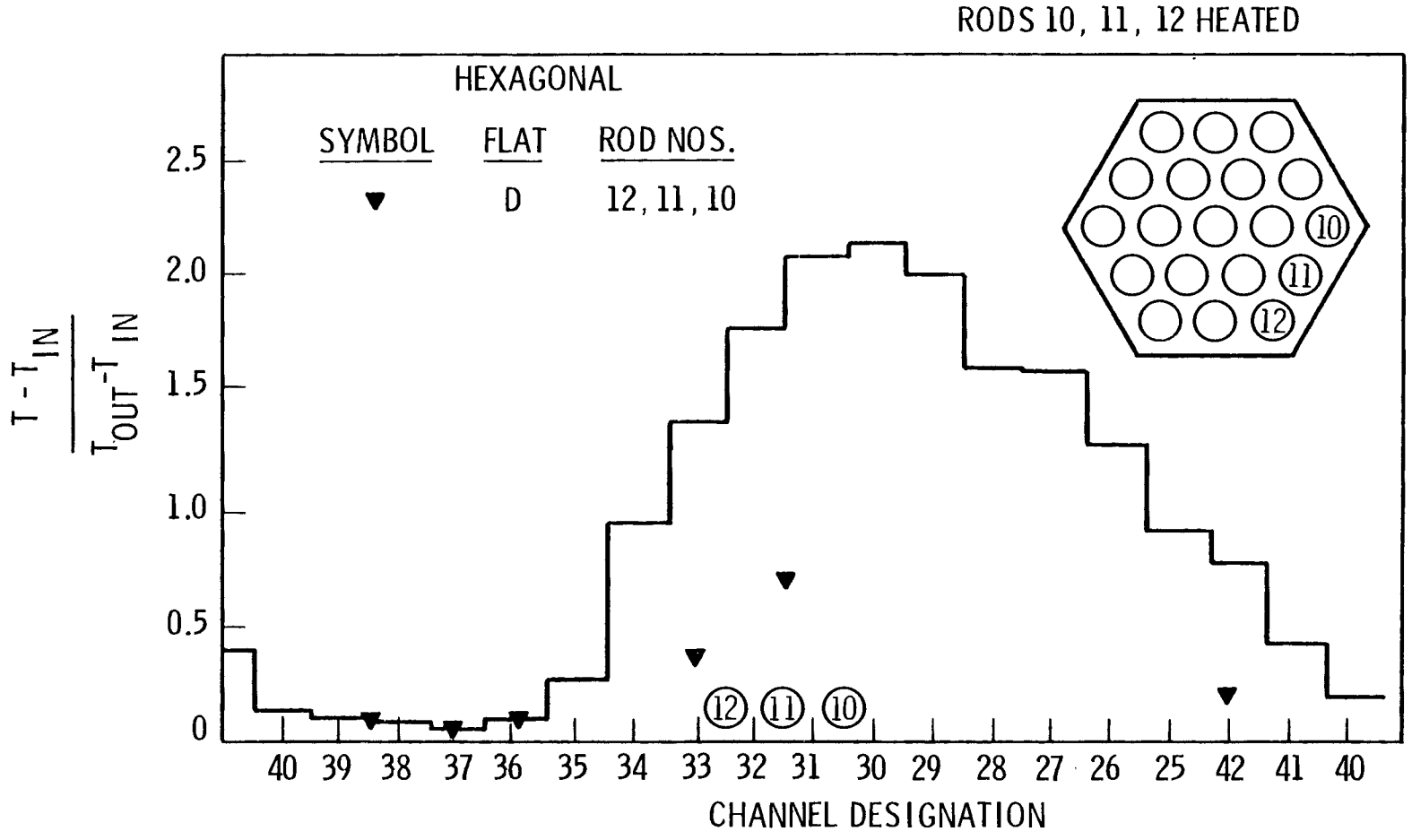

FIGURE 15. Peripheral Subchannel Temperatures (X = 18 in.)

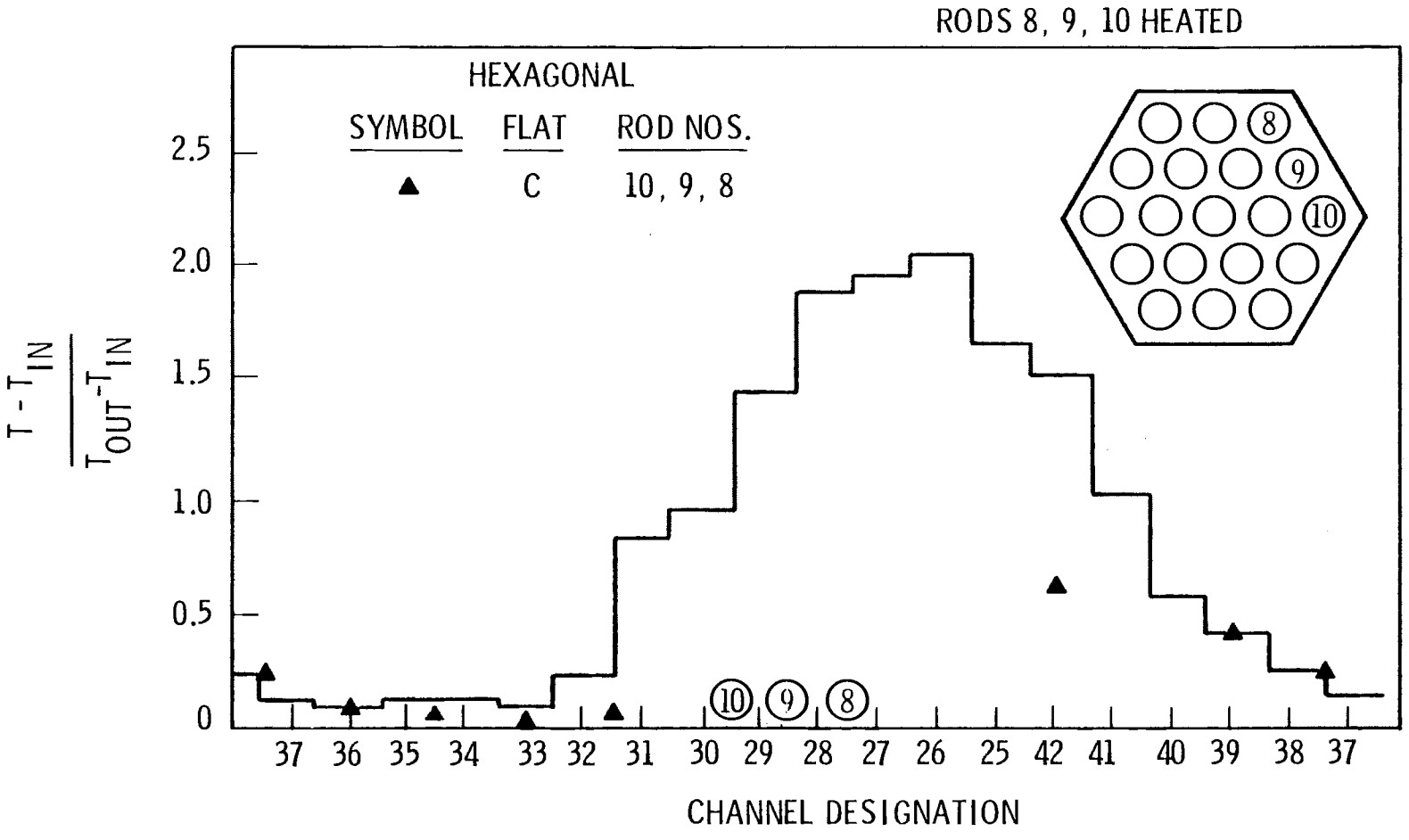

FIGURE 16. Peripheral Subchannel Temperatures (X = 18 in.)

CONCLUSIONS

The COBRA-IV computer code, using the modifications to the standard wire wrap model discussed in Chapter 2, has successfully modeled the thermal-hydraulics of experimental simulations of wire wrapped fuel assemblies. Some conclusions can be made with respect to areas in which the code is currently successful and areas in which further improvements are needed.

The area of the code's greatest success appears to be the ability to model the hydrodynamics of the wire wrap assemblies. This is evidenced by the agreement of the COBRA results with the velocities and pressures measured in the MIT and French experiments. Additional supporting evidence may be inferred from the results of the ANL salt and dye injection experiments.

The data comparisons relevant to modeling energy transport are somewhat ambiguous. Excellent agreement between the data and COBRA code was obtained for the ORNL exit rake temperature measurements (Figure 8) while the agreement between theory and data for the duct wall temperature measurements varied from "good" to "not so good", (see Figures 9 and 11 through 16). An attempt was made to improve the overall agreement by varying peripheral subchannel areas and gap widths in the code to account for the observed bundle distortion,[5] but these efforts were only marginally successful.

Another problem encountered in the modeling of energy transport was the previously mentioned "flattening" of enthalpy (or salt) concentrations due to the use of upwind differencing in the numerical algorithm. This effect is most apparent in the ANL salt injection experiments (see Figures 1 and 2), where the computed salt concentration profiles are much "flatter" than the experimental concentrations. An attempt to minimize the numerical diffusion by enthalpy averaging between donor and acceptor subchannels resulted in an unstable solution for the energy equation.

In summary, the investigation found that the COBRA-IV code can successfully model the hydrodynamics of a wire wrap fuel assembly. Additional efforts should be made to improve enthalpy transport modeling techniques currently in the code.

REFERENCES

1. J. J. Lorenz, D. R. Pedersen and R. D. Pierce, Peripheral Flow Visualization Studies in a 91-Element Bundle. ANL-RAS-73-14, Argonne National Laboratory, Argonne, IL, June 1973.

2. D. S. Rowe, COBRA-IIIC: A Digital Computer Program for Steady-State and Transient Thermal-Hydraulic Analysis of Nuclear Fuel Elements. BNWL-1695, Battelle, Pacific Northwest Laboratories, Richland, WA, March, 1973.

3. J. J. Lorenz, T. Gensberg and R. A. Morris, Experimental Mixing Studies and Velocity Measurements With a Simulated 91-Element LMFBR Fuel Assembly. ANL-CT-74-09, Argonne National Laboratory, Argonne, IL, March 1974.

4. Y. B. Chen, K. Ip and N. E. Todreas, Velocity Measurements in Edge Subchannels of Wire Wrapped LMFBR Fuel Assemblies. COO-2245-11TR, Department of Nuclear Engineering, Massachusetts Institute of Technology, Cambridge, MA, September 1974.

5. M. H. Fontana, Temperature Distribution in the Duct Wall and at the Exit of a 19-Rod Simulated LMFBT Fuel Assembly (FFM Bundle 2A). ORNL-4852, Oak Ridge National Laboratory, Oak Ridge, TN, April 1973.

6. J. Lafay, B. Menant and J. Barrois, "Influence of Helical Wire Wrap Spacer System in a 19-Rod Bundle." Presented to the 1975 Heat Transfer Conference, San Francisco, CA, April 1975.

7. E. H. Novendstern, "Turbulent Flow Pressure Drop Model for Fuel Rod Assemblies Utilizing a Helical Wire Wrap Spacer System." Nuclear Engineering and Design 22: 19-27, 1972.

DISTRIBUTION

No. of Copies

U.S. Department of Energy
A. A. Churm
Chicago Patent Group
Argonne, IL 60439

27 DOE Technical Information Center

Argonne National Laboratory
Director, Components Technology
9700 S. Cass Avenue
Argonne, IL 60439

Argonne National Laboratory
R. Singer
9700 S. Cass Avenue
Argonne, IL 60439

Argonne National Laboratory
P. Betten
9700 S. Cass Avenue
Argonne, IL 60439

Atomics International
J. Vitti
PO Box 309
Canoga Park, CA 91304

Babcock and Wilcox
W. Bingham
PO Box 1260
Lynchburg, VA 24502

Combustion Engineering
R. Noyes
1000 Prospect Hill Road
Windsor, CN 06095

Electric Power Research Institute
R. Sehgal
PO Box 10412
Palo Alto, CA 94303

No. of Copies

Electric Power Research Institute
K. Sun
PO Box 10412
Palo Alto, CA 94303

U.S. Department of Energy
Assistant Director for Materials
Germantown, MD 20767

U.S. Department of Energy
Assistant Director for Engineering
Germantown, MD 20767

U.S. Department of Energy
Assistant Director for Reactor Safety
Chief, Safety Analysis Branch
Germantown, MD 20767

U.S. Department of Energy
Chief, Fuel Systems Branch
Germantown, MD 20767

U.S. Department of Energy
Chief, Engineering Component Branch
Germantown, MD 20767

U.S. Department of Energy
Reactor Analysis Branch
R. J. Neuhold
Germantown, MD 20767

General Electric Company
K. Horst
310 DeGuigne Drive
PO Box 5020
Sunnyvale, CA 91304

Massachusetts Institute of Technology
N. Todreas
77 Massachusetts Avenue
Cambridge, MA 02139

No. of Copies

Oak Ridge National Laboratory
C. Wilson
CRBRP Project Office
Oak Ridge, TN 37830

Oregon State University
L. Peddicord
Corvallis, OR 97331

Rensselaer Polytechnic Institute
Department of Nuclear Engineering
R. Lahey
Troy, NY 12181

University of Pittsburgh
A. Bishop
Pittsburgh, PA 15261

10 Westinghouse Electric Corporation
Advanced Reactors Branch
R. Markley
Waltz Mill Site
Box 158
Madison, PA 15663

Westinghouse Electric Corporation
Advanced Reactors Branch
E. Novendstern
Waltz Mill Site
Box 158
Madison, PA 15663

Westinghouse Electric Corporation
Advanced Reactors Branch
B. Vegter
Waltz Mill Site
Box 158
Madison, PA 15663

ONSITE

DOE Richland Operations Office

H. E. Ransom

No. of Copies

Westinghouse Hanford Company
Hanford Engineering Development Laboratory

R. Bennett
E. Evans
J. Hanson
J. Muraoka

Pacific Northwest Laboratory

K. L. Basehore
J. M. Bates
J. M. Creer
25 T. L. George
E. U. Khan
W. A. Prather
A. M. Sutey
D. S. Trent
C. L. Wheeler
Technical Information (5)
Publishing Coordination (2)